08.2

Formation of InAs$_{1-x}$N$_x$ islands and InAs stem-assisted InAs$_{1-x}$N$_x$ nanowires by means of epitaxial growth on silicon

© A.K. Kaveev [1], D.V. Miniv [2], V.V. Fedorov [2]

[1] Ioffe Institute, St. Petersburg, Russia
[2] Alferov Federal State Budgetary Institution of Higher Education and Science, Saint Petersburg National Research Academic University of the Russian Academy of Sciences, St. Petersburg, Russia
E-mail: kaveev@mail.ioffe.ru

The possibility of forming InAs$_{1-x}$N$_x$ nanowires on InAs stems on the Si(111) surface coated with partly destructed silicon oxide was demonstrated. Formation of parasitic islands was also detected. It was revealed that in the first case the predominantly wurtzite structural phase is formed, while in the second case the sphalerite structural phase dominates.

Keywords: InAs$_{1-x}$N$_x$, dilute nitride, nanowires, molecular beam epitaxy.

InAs-based nanowires (NWs) are an attractive material in view of their applicability in the field of infrared photonics and photodetection [1,2]. A significant surface/volume ratio makes possible epitaxial growth of materials with a noticeable mismatch of lattice parameters, for instance, ensures growth of A$_3$B$_5$ materials on silicon [3]. Applying NWs in infrared photodetection allows a reduction in the detector active region volume and, hence, in the dark current [4,5]. Self-induced InAs NWs tend to crystallize in the metastable wurtzite (WZ) structure with the bandgap wider than that in the case of the zinc blende (ZB) structure which is stable in bulk InAs crystals [6]. The photoresponse range of photodetectors based on InAs NWs may be extended by implanting antimony [7] or nitrogen [8,9]. Stabilization of dilute solid solutions InAs$_{1-x}$N$_x$ is in general hindered by phase segregation and competitive implantation of group V atoms [10]. This problem may be overcome by creating InAs$_{1-x}$N$_x$ NWs since the number of NW elastic stresses is lower due to a more favorable surface/volume ratio, i.e. a more developed heterointerface, which makes more pronounced the effect of epitaxial stabilization of solid solutions. Epitaxial stabilization of InAs$_{1-x}$N$_x$ was demonstrated in planar heterostructures [11,12].

This study has demonstrated the possibility of forming the InAs$_{1-x}$N$_x$ nanostructures of various morphologies on the SiO$_x$/Si(111) substrates. Those structures are islands and InAs$_{1-x}$N$_x$ NWs grown via the self-induced mechanism. For this purpose there was used a Veeco GEN III molecular beam epitaxy system equipped with an In effusion cell, As cracker source, and source of inductively coupled nitrogen plasma. The nitrogen flow was 0.9 ml/min at the source power of 350 W. Formation of silicon oxide on Si substrates was performed by the modified Chiraki method [13]. To facilitate the nucleation, the substrates were subjected to thermal annealing in ultrahigh vacuum in order to create point

defects in the silicon oxide layer [14], i.e. to make the oxide layer partially destructed. The crystalline structure of the samples was studied by X-ray diffraction analysis (XRD). Therewith, there were constructed reciprocal space maps obtained by 3D fitting of individual images corresponding to specific azimuthal angles the sample was installed at.

The InAs$_{1-x}$N$_x$ NWs were obtained by forming on InAs stems at the growth temperature of 460°C and equivalent flow pressure ratio As$_4$/In of 90. The ratio between the InAs$_{1-x}$N$_x$ and InAs stem growth times was 4.5. Fig. 1, *a* presents a scanning electron microscopy (SEM) lateral projection image of an array of InAs stems arising at the places of silicon oxide thermal destruction. In the absence of InAs NW stems, the direct growth of InAs$_{1-x}$N$_x$ led to a predominance of the 3D island growth over the NW growth (Fig. 1, *b*). The InAs$_{1-x}$N$_x$ NW surface density was extremely insignificant ($< 0.5 \mu$m^{-2}), as well as the NW mean height (< 400 nm). The InAs$_{1-x}$N$_x$ islands got formed directly on the silicon oxide layer, which may be explained by an increase in the probability of InAs$_{1-x}$N$_x$ nucleation in the presence of reactive nitrogen species [15]. We failed to achieve a significant number of InAs$_{1-x}$N$_x$ NWs without using at least stems of InAs NWs; at the same time, using stems made it possible to create longer NWs. Figure 1, *c* illustrates the result of growing InAs$_{1-x}$N$_x$ on InAs stems (the insets present the NW top view and schematic representation). The InAs$_{1-x}$N$_x$ NW mean height and diameter are $1.2 \pm 0.3 \mu$m and 110 ± 30 nm, respectively. For comparison, these values in the case of InAs stems are $0.5 \pm 0.2 \mu$m and 90 ± 50 nm. As shown by the SEM image (top view) presented in the Fig. 1, *c* right inset, growth of the InAs$_{1-x}$N$_x$ NWs on InAs stems is in addition accompanied by parasitic growth of 3D islands. If, however, undamaged silicon oxide is used, the island layer becomes continuous and completely covers the oxide surface.
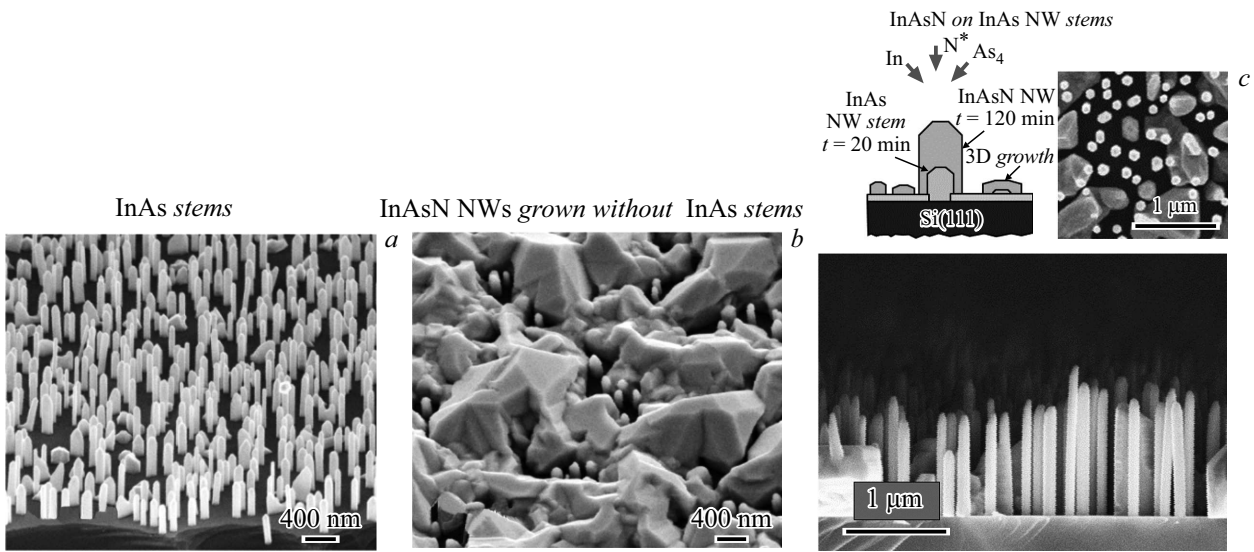
Figure 1. *a* — SEM images of InAs stems in the lateral projection; *b* — SEM image of an $InAs_{1-x}N_x$ NW array grown free of InAs stems directly on the annealed $SiO_x/Si(111)$ surface; *c* — SEM images of $InAs_{1-x}N_x$ NWs grown on InAs stems in the lateral and vertical (right inset) projections.
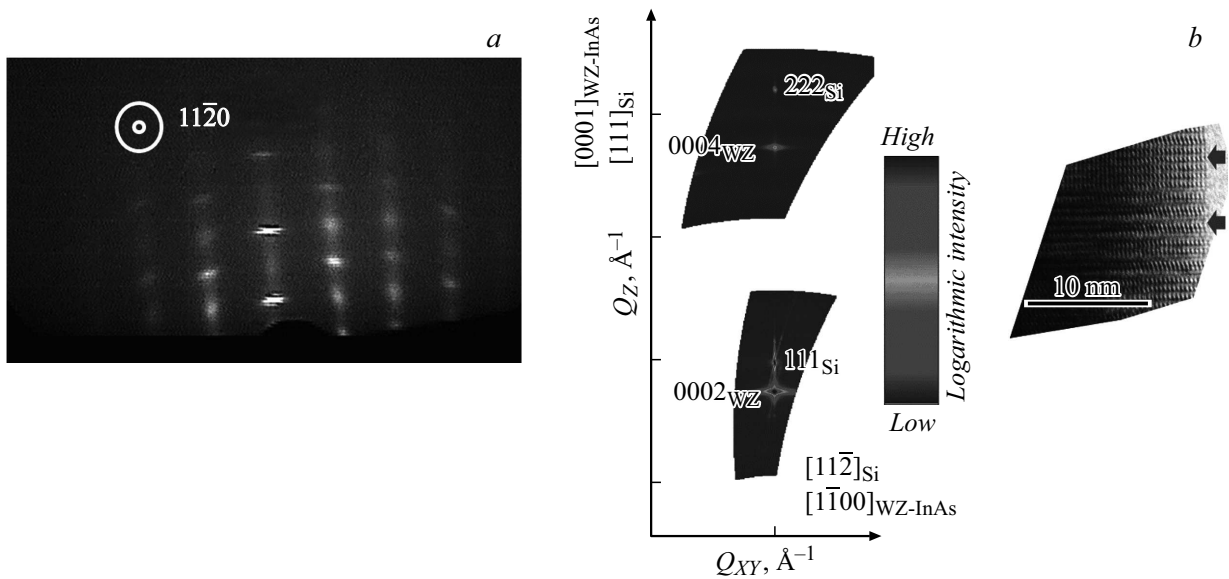
Figure 2. *a* — typical FED pattern for $InAs_{1-x}N_x$ NWs. *b* —a fragment of the zero-order $\langle\bar{1}\bar{1}20\rangle$ Laue zone for $InAs_{1-x}N_x$ NWs. Positions of Bragg reflections for the $InAs_{1-x}N_x$ wurtzite phase and silicon are marked. The right panel demonstrates a TEM image; the upper arrow indicates the area of defect free wurtzite structure, the lower arrow indicates the packing phase disorder.

The XRD measurements and analysis of the reciprocal space patterns have shown that $InAs_{1-x}N_x$ NWs form a wurtzite-type crystalline phase similar to that for InAs NWs. These measurements are in agreement with reflection high energy electron diffraction (HEED) patterns (Fig. 2, *a*) and also with those typical of the wurtzite phase of InAs NWs in the electron beam direction $[11\bar{2}0]$ (see [16]). We have found epitaxial relations of the grown NW arrays: NW growth direction [0001] is oriented along the Si direction [111], while in the substrate plane the $[11\bar{2}0]$ direction of the InAs wurtzite lattice is oriented along the $[1\bar{1}0]$ Si lattice direction. Figure 2, *b* presents a fragment of the zero-order $\langle\bar{1}\bar{1}20\rangle$ Laue zone obtained for the sample of $InAs_{1-x}N_x$ NWs. Reflections associated with the sphalerite phase are poorly pronounced. The figure's right panel presents a high-resolution transmission electron microscopy (TEM) pattern of NW. In the pattern, the upper arrow indicates a region of the defect-free wurtzite structure, while the lower arrow indicates a case of the packing phase disorder. This pattern as a whole confirms the wurtzite phase formation in NWs.
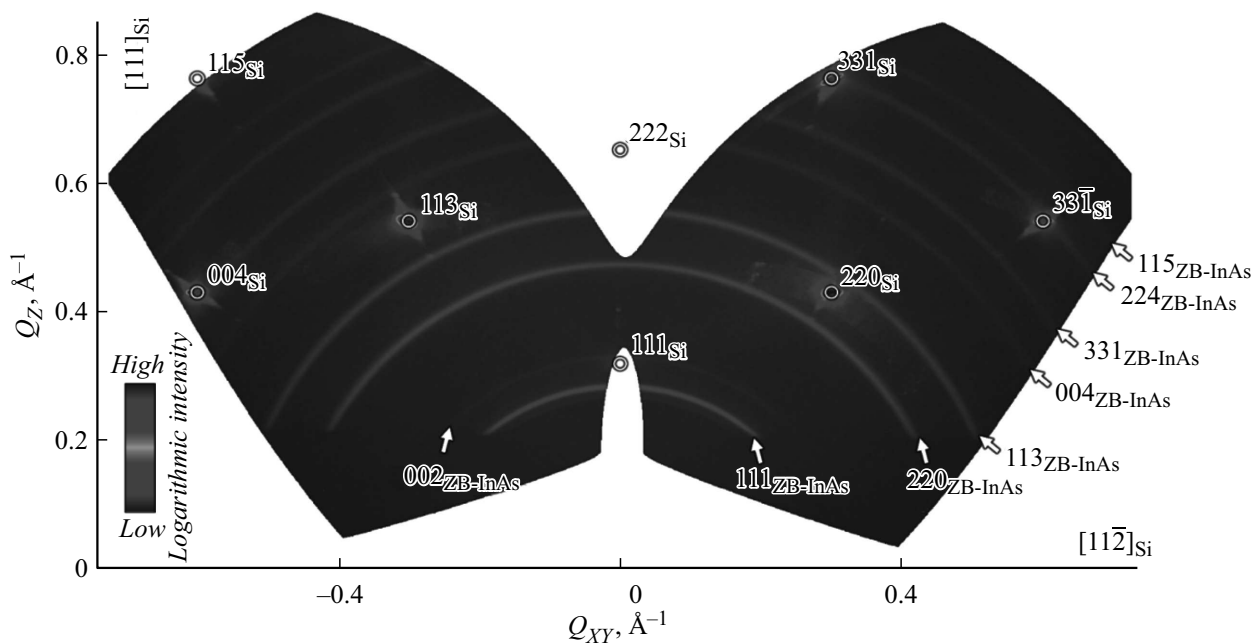
Figure 3. A fragment of the zero-order $\langle 1\bar{1}0\rangle$ Laue zone of silicon. Model positions of Bragg reflections in Si are marked by circles. The arrows indicate the diffraction circles corresponding to the polycrystalline InAs sphalerite phase.

To assess the structural properties of parasitic 3D islands, an NW-free sample was studied. The island layer has a disordered sphalerite-type structure characteristic of bulk InAs crystals. The X-ray diffraction patterns exhibit a single set of continuous diffraction circles. A typical two-dimensional cross section demonstrating a fragment of the silicon zero-order $\langle 1\bar{1}0\rangle$ Laue zone is presented in Fig. 3. The observed diffraction circles can be attributed to the cubic crystal structure of sphalerite. No extra diffraction circles specific for the wurtzite structure characteristic of the InAs NWs were detected. Those extra rings would correspond to diffraction from the $\{1\bar{1}0l\}$ and $\{2\bar{2}0l\}$ crystallographic planes.

The nitrogen concentration was assessed by secondary ion mass spectrometry (SIMS). The nitrogen amount was approximately estimated as 0.5 at.%. Thus, the study has demonstrated the possibility of both the island-type growth of the InAs$_{1-x}$N$_x$ sphalerite phase and growth of the wurtzite phase of InAs$_{1-x}$N$_x$ NWs. The latter was formed in case of using the InAs stem. The proposed InAs$_{1-x}$N$_x$ NW arrays are a promising material for creating photodetectors and light-emitting devices operating in the near— and mid IR ranges.

Conflict of interests

The authors declare that they have no conflict of interests.

References

[1] A. Abrand, M.A. Baboli, A. Fedorenko, S.J. Polly, E. Manfreda-Schulz, S.M. Hubbard, P.K. Mohseni, ACS Appl. Nano Mater., **5**, 840 (2022). DOI: 10.1021/acsanm.1c03557.

[2] X. Zhang, H. Huang, X. Yao, Z. Li, C. Zhou, X. Zhang, P. Chen, L. Fu, X. Zhou, J. Wang, W. Hu, W. Lu, J. Zou, H.H. Tan, C. Jagadish, ACS Nano, **13**, 3492 (2019). DOI: 10.1021/acsnano.8b09649.

[3] W.G. Schmidt, Appl. Phys. A, **75**, 89 (2002). DOI: 10.1007/s003390101058

[4] R.C. Jones, in *Advances in electronics and electron physics*, ed. by L. Marton (Academic Press, 1953), vol. 5, p. 1–96. DOI: 10.1016/S0065-2539(08)60683-6

[5] Z. Li, J. Allen, M. Allen, H.H. Tan, C. Jagadish, L. Fu, Materials, **13**, 1400 (2020). DOI: 10.3390/ma13061400

[6] S. Pournia, S. Linser, G. Jnawali, H.E. Jackson, L.M. Smith, A. Ameruddin, P. Caroff, J. Wong-Leung, H.H. Tan, C. Jagadish, H.J. Joyce, Nano Res., **13**, 1586 (2020). DOI: 10.1007/s12274-020-2774-0

[7] T. Xu, H. Wang, X. Chen, M. Luo, L. Zhang, Y. Wang, F. Chen, C. Shan, C. Yu, Nanotechnology, **31**, 294004 (2020). DOI: 10.1088/1361-6528/ab8591

[8] A. Krier, M. de la Mare, P.J. Carrington, M. Thompson, Q. Zhuang, A. Patané, R. Kudrawiec, Semicond. Sci. Technol., **27**, 094009 (2012). DOI: 10.1088/0268-1242/27/9/094009

[9] H. Naoi, Y. Naoi, S. Sakai, Solid-State Electron., **41**, 319 (1997). DOI: S0038-1101(96)00236-5

[10] W. Walukiewicz, J.M.O. Zide, J. Appl. Phys., **127**, 010401 (2020). DOI: 10.1063/1.5142248.

[11] Q. Zhuang, A.M.R. Godenir, A. Krier, K.T. Lai, S.K. Haywood, J. Appl. Phys., **103**, 063520 (2008). DOI: 10.1063/1.2896638.

[12] J. Ibanez, R. Oliva, M. De la Mare, M. Schmidbauer, S. Hernandez, P. Pellegrino, D.J. Scurr, R. Cusco, L. Artus, M. Shafi, R.H. Mari, M. Henini, Q. Zhuang, A. Godenir, A.J. Krier, Appl. Phys., **108**, 103504 (2010). DOI: 10.1063/1.3509149.

[13] W.J. Kern, Electrochem. Soc., **137**, 1887 (1990). DOI: 10.1149/1.2086825

[14] G. Koblmuller, S. Hertenberger, K. Vizbaras, M. Bichler, F. Bao, J.-P. Zhang, G. Abstreiter, Nanotechnology, **21**, 365602 (2010). DOI: 10.1088/0957-4484/21/36/365602

[15] M. Gruart, G. Jacopin, B. Daudin, Nano Lett., **19**, 4250 (2019). DOI: 10.1021/acs.nanolett.9b00023.

[16] J. Jo, Y. Tchoe, G.-C. Yi, M. Kim, Sci. Rep., **8**, 1694 (2018). DOI: 10.1038/s41598-018-19857-2.

Translated by EgoTranslating